Superimposed Non Interfering Probes to extend the Phase Doppler Anemometry size range

By

Fabrice Onofri*, Anne Lenoble* and Stefan Radev**

*Institut Universitaire des Systèmes Thermiques Industriels,
UMR CNRS 6595-Université de Provence
Technopôle de Château-Gombert, 13008 Marseille cedex 13, France

** Institute of Mechanics
Bulgarian Academy of Sciences,
ul. "Acad. G. Bonchev" bl. 4, 1113 Sofia, Bulgaria

ABSTRACT

In classical phase Doppler systems three detectors are commonly used to determine the particles size whatever, basically, this technique requires only two detectors. The third detector is in fact mainly used to overcome the 2π ambiguity on phase-shift measurements.

In the present work an alternative solution is introduced which allows to keep the same accuracy and dynamic range of the size measurements without requiring a third detector. The basic idea of the proposed solution is to superimpose two (or more) probe volumes of the same wavelength but with different beams angles (i.e. fringes spacing). Thus, the Doppler signals produced by a particle moving in the probe volume exhibit simultaneously two Doppler frequencies. The signal phase-shift is different at each of these frequencies. As the phase-shift diameter conversion factor increases with the beam angle, one phase-shift measurement can be used to keep the size dynamic range and the other one, to increase the accuracy on the size determination.

The first key point of this technique is to avoid interference phenomena between the different pairs of laser beams used to produce the superimposed probes. In the case there is interference, it is shown that the probe volume fringes pattern seems actually to be too complex for sizing or velocimetry applications. So in the present work several solutions to produce Superimposed Non Interfering Probes (SNIP) are investigated: *i)* a single low coherence laser source with a retardation line, *ii)* two independent laser sources as a limit case of the previous one and finally, *iii)* a single laser source and cross-polarized probes.

The second key point to be solved is the signal processing scheme. In the present work the principle and the relevance of a signal processing scheme based on the calculation of the cross spectral density function of SNIP-PDA signals is clearly established.

The principle of the proposed technique is validated with different experimental tests carried out on flowing spherical glass beads and fixed metallic wires. The preliminary results have shown already that for both types of particles a SNIP-PDA with only two superimposed probes has already the same resolution than a classical PDA system.

1 INTRODUCTION

Phase Doppler Anemometry (PDA) is now a well established interferometric technique for particle size and velocity measurement in two-phase flows. Since the introduction of its principle, almost 25 years ago, two types of models are used to explain the basis of this technique. The first model called the "scattered fields addition model" is a rigorous approach based on the exact calculation of the interference field produce onto the detectors aperture by the net field scattered by the particle located at the crossing of two laser beams. The particle scattering properties are calculated with either geometrical optics or the Lorenz-Mie Theory. The second model called the "heuristic fringes model" was first introduced to explain the basis of the Laser Doppler Anemometry (LDA), see for instance Durst et al. 1981. Afterwards, it has been used to explain the basics of PDA as this technique is an extension of the LDA.

In the heuristic fringes model it is considered that at the crossing of two incident coherent laser beams there exists a fringes pattern whose characteristics depends only on the laser beams properties (wavelength, beam waist and crossing angle). The particle is then assumed to be perfectly spherical and to act as a micro spherical lens that project the fringes pattern observed at the beams crossing (i.e. probe volume) onto the detectors aperture, see Fig 1. Thus, the projected fringes pattern depends on the particle properties (size and refractive index) and the characteristics of the incident laser beams. From this simple model the dependence between the particle size and the measured phase-shift can be deduced simply as bellow.

In the paraxial approximation, i.e. for rays always very close and nearly parallel to the optical axis, the spherical particle focal length is equal to $f=mR/[2(m-1)]$ (we restrict our analysis to the refracted rays only), where R is the particle radius, m its relative refractive index for the laser wavelength l and f, its equivalent focal length. In the probe volume the fringes pattern is defined by the fringes spacing, $i_v=sin(l)/[2sin(a/2)]$, where a is the half-beams angle. For a projection plan located at distance L from the particle focal point, the projected fringes spacing becomes, $i_p=i_vL/f$. For two identical point detectors D_1 and D_2, symmetrical to the (Oz) axis with elevation angles $\psi_1=\psi$, $\psi_2=-\psi$, the distance between the detectors is of $l_{12}=tan(2y)L$. When a particle moves perpendicularly to the fringes of the probe volume the projected fringes move periodically onto the detectors aperture too. So that the detectors observe the same periodic signal but with a phase delays $Df_{12}=2p(l_{12}/i_p)=2p(l_{12}/i_vL)f$. This phase delay or "phase-shift" is a linear function of the particle diameter and its slope namely, the phase-diameter conversion factor, is equal to $C_{12}=Df_{12}/(2R)$ with

$$C_{12}=\frac{p}{l}\frac{m}{m-1}\tan(y_1-y_2)\sin(a)\ [rad/\mu m] \qquad [1]$$

The validity of Eq. 1 is limited to the paraxial approximation ($\psi\approx0°$) and it does not take into account of many effects such as diffraction, polarization and reflection of the rays… Nevertheless this drastically simple equation gives a good estimation of the dependency of C with parameters y, a, m. A numerical evaluation of the validity of Eq. 1 was made in comparison with the predictions of a full geometrical optics interference model (Naqwi and Durst 1991). We found that C is estimated with an accuracy better than *2.5%* for the parameters range $y\ \hat{I}\pm[0\text{-}5]$, $a\ \hat{I}\ [0\text{-}12°]$, $m\hat{I}\ [1.1\text{-}1.7]$. It must be pointed out that even if the heuristic model is not the correct physical and mathematical way to describe the PDA basic principle it represents a simple and efficient tool to describe the main features of this technique and to bring new ideas.

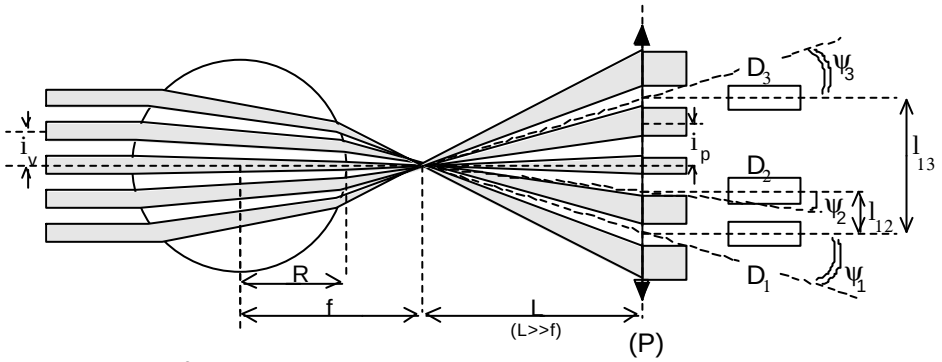

Figure 1 Principle of the Phase Doppler Anemometry technique according to the heuristic fringes model. In this model the particle acts as a projection system for the probe volume fringes. The projected fringes spacing can be simply related to the particle size.

When all the optical parameters of the experimental setup and the particle refractive index m are known, one can easily deduce the particle diameter: $D=Df_{12}/C_{12}$ from Eq. 1 and the measurement of the phase-shift Df_{12}.
In fact, the particle diameter is deduced from a phase-shift measurement which possesses a priori a $2p$ indetermination. So that the particle diameter reads normally $D=(Df_{12}+n2p)/C_{12}$ where n is a natural integer which has to be determined as well. To limit this so-called "2π ambiguity" effect a third detector is often used. It

allows the determination of two phases shifts, Df_{12} and Df_{13} for each measured particle. The location of the additional detector D_3 is chosen typically to meet the condition $C_{12}/C_{13}»3$ (i.e. $l_{12}/l_{13}»3$, see Fig. 1). This solutions allows to keep the sensibility of the phase-shift to the particle size and to obtain a reasonable dynamic of the size range (three times higher than with C_{12}) that can be measured.

The use of a third detector, is now well established and most of the commercial PDA systems have adopt it. Nevertheless, it may be unusable for some applications and more particularly when a large conversion factor is required to size for instance, very small droplets or fibers. It is also not very effective for other purposes like particle non sphericity and trajectory effects detection [Tropea et al., 1996]. It might not be also the most effective solution for the diagnosis of irregular particles [Naqwi 1996, Onofri 2000].

In the present work an alternative solution is introduced to overcome the use of a third detector. It uses superimposed multiple probes volumes with different fringes spacing, as shown in Fig. 2 where its principle according to the heuristic fringes model is sketched. In this configuration the particle still acts as a projection system but now, the fringes pattern projected onto the detectors apertures, and then the electric output signal from detectors, exhibit a multiple frequency structure during the particle motion in the probe volume. The low frequency modulation (Doppler frequency) corresponds to a large fringes spacing, i.e. a small beam angle which leads to a small conversion factor (see Eq. 1). The high frequency modulation (Doppler frequency) corresponds to a smaller fringes spacing, i.e. to a larger beam angle and then to a higher conversion factor. The idea is then to measure the phase-shift between the two PDA signals (coming from detectors D_1 and D_2) at each Doppler frequency presented in the signals so that we are able to measure two phase-shifts with only two detector and this for each particle crossing the probe volume.
Fig. 2 sketches the projection by a spherical particle of two superimposed fringes pattern. In the probe volume the two fringes spacing are in the ratio $i_{v2}/i_{v1}=2$. The projected fringes are in the same ratio, $i_{p2}/i_{p1}=2$. For small beams angles, the conversion factors are also (see Eq. 1) in the same ratio. $C_{12}(i_{p1})/C_{12}(i_{p2})»2$.

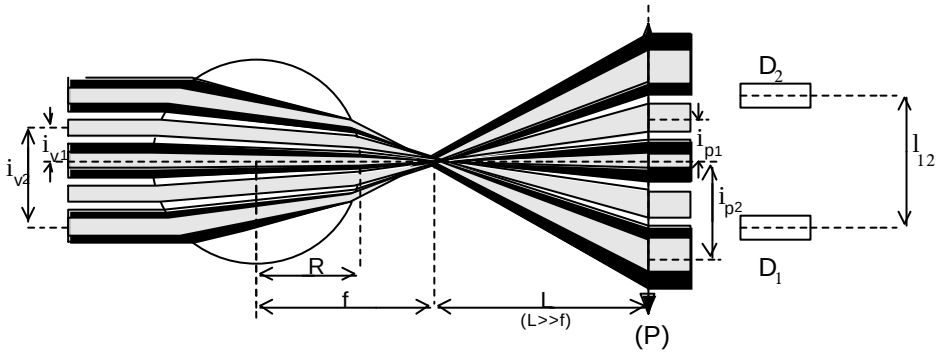

Figure 2 Principle of the Superimposed Non Interfering Probes - Phase Doppler Anemometry (SNIP-PDA) according to the heuristic fringes model. For each fringes pattern in the probe volume, the PDA signals exhibit different Doppler frequencies and phase-shifts.

The principle of this technique consist of two key points: to avoid mutual interferences between each pair of laser beams used to produce the probe volumes and the signal-processing scheme of experimental signals. Due to the first condition to be fulfilled, this technique will be referenced further on as the Superimposed Non Interfering Probes - Phase Doppler Anemometry (SNIP-PDA). This paper is organized as follows. Section 2, reviews different possibilities and conditions to produce non-interfering superimposed PDA probe volumes. Section 4 presents the signal-processing scheme developed to recover the multiple phase-shifts and Doppler frequencies from SNIP-PDA signals. Section 5, presents the experimental setups and results carried out to demonstrate the applicability of the proposed technique. Section 6, we discuss the most interesting features of the SNIP-PDA and the perspectives for future improvements and developments.

2 METHODS TO OBTAIN NON INTERFERING SUPERIMPOSED PROBE VOLUMES

2.1 Superimposition of multiple coherent beams pairs

We are interested here to calculate the interference field produced by the superimposition of $2N$ (N is a natural integer) crossing pairs of laser beams which propagates in the (Oxz) plane, see Fig. 2. To simplify this analysis the laser beams are considered as coherent linearly polarized local plane waves, so that the corresponding electric field vector of the beam n reduces to:

$$\mathbf{E}_n = E_0 e^{-j(\mathbf{k}_n.\mathbf{r}+j_n)} e^{-j2pnt} \qquad [2]$$

where $\boldsymbol{r}$ is the position vector in the coordinate system *(Oxyz)* and, $\mathbf{k_n}$, φ_n and ν, are the wave vector, the phase and frequency of beam *n* respectively, see Fig. 3. Wave vectors $\mathbf{k_{2l-1}}$ and $\mathbf{k_{2l}}$, where *l* is a positive natural integer, are symmetrical in respect to (Oz) axis. Angles α_{2l-1} and α_{2l} denote the angle between the wave vectors k_{2l-1}, k_{2l} and the reference direction (Oz) respectively. All beams are considered to be linearly polarized with the same state of polarization.

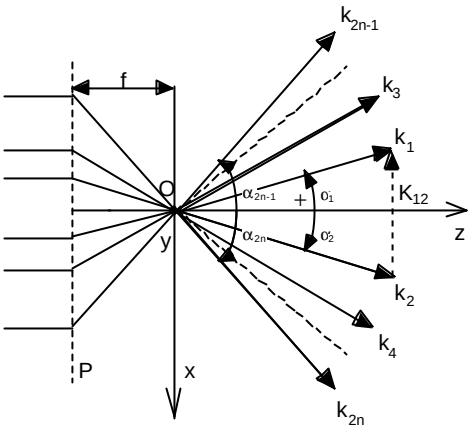

Figure 3 Coordinate system (Oxyz) at the beams crossing location

The net field amplitude is a sum of all of the component fields and the resulting field intensity is the time average (over a period much longer than 1/ν) of the modulus squared of the total amplitude:

$$\langle I \rangle_{1/n} \propto \left\langle \left| \sum_{n=1}^{2N} \mathbf{E}_n \right|^2 \right\rangle = \left\langle \sum_{n=1}^{2N} \mathbf{E}_n \sum_{n=1}^{2N} \mathbf{E}_n^* \right\rangle \qquad [3]$$

with $\mathbf{K}_{nm} = \mathbf{k}_n - \mathbf{k}_m$ the resulting field intensity is

$$\langle I \rangle_{1/n} \propto E_0^2 \left(N + 2 \sum_{n=1}^{2N} \sum_{m>n}^{2N} \cos(\mathbf{K}_{nm}.\mathbf{r} + j_{nm}) \right) \qquad [4]$$

In the coordinate system *(Oxyz)* the general expression for the scalar product $\mathbf{K}_{nm}\mathbf{r}$ reads for *n=1…2N* and *m>n*,

$$\mathbf{K}_{nm}.\mathbf{r} = \frac{2p}{l} \begin{pmatrix} \cos(a_n) - \cos(a_m) \\ \sin(a_n) - \sin(a_m) \end{pmatrix} \begin{pmatrix} z \\ x \end{pmatrix} \qquad [5]$$

where $j_{nm} = j_n - j_m$ is the phase delay between beams *n* and *m* compared to the reference plane *(P)*. In plane (P) distant of *f* from the co-ordinate system center *(O)*, all beams are assumed considered to be in phase,

$$j_{nm} = \frac{2pf}{l} \left(\frac{1}{\cos(a_n)} - \frac{1}{\cos(a_m)} \right) \qquad [6]$$

In Eq. 4 the cosine term corresponds to the classical fringes pattern observed in a PDA probe volume when two coherent beams cross each other. In Eq. 5 the scalar product is function of *x* only when *n=2l-1* and *m=2l* (for symmetrical beams in respect to the *(0z)* axis, i.e. the fringes are parallel to *(Oz)* as in classical PDA probes). It is

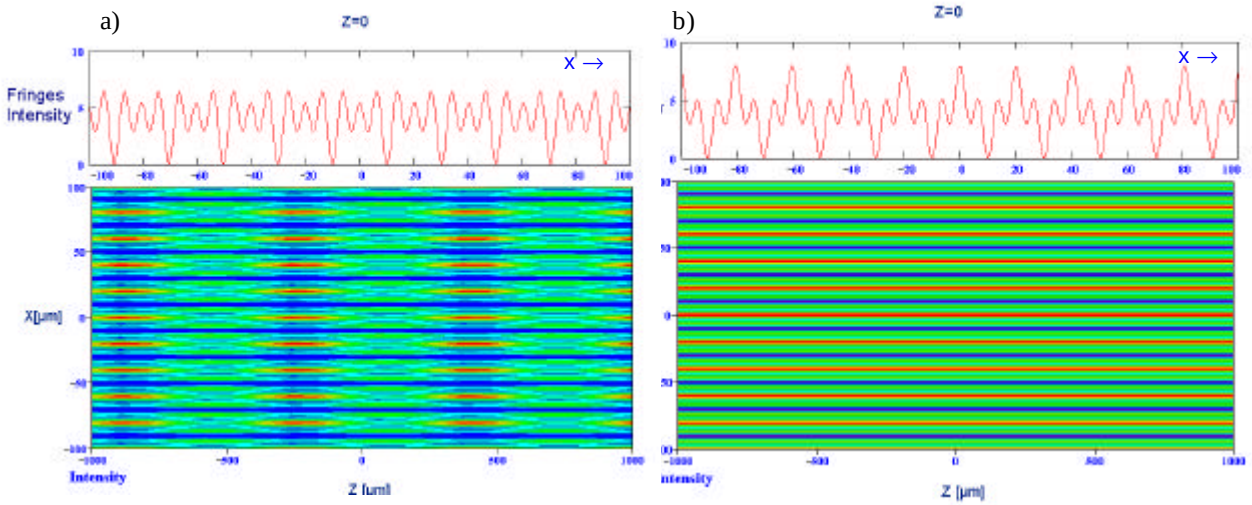

Figure 4 Calculation of the fringes pattern in the (Oxy) plane when a) two coherent beam pairs are superimposed and b) when two incoherent or cross-polarized beam pairs are superimposed, with l=0.6328µm, a_p/a_q=3.

a function of both x and z in other cases (i.e. the fringes are parallel to the bisector of the directions $\mathbf{k_n}$ and $\mathbf{k_m}$). In the last case the net field intensity is much more complex than the one observed in a classical LDA/PDA probe, see Fig 4a).

Fig 4 a) shows the fringes pattern produced by the interference of two coherent pairs of laser beams ($2N=4$). Eqs. 4-6 were used here for the laser wavelength $l=0.6328\mu m$, a distance $f=0.5m$ to the reference plane (i.e. a lens for instance) and for the beam angles $a_1=-a_2=0.9°$ with $a_3=-a_4=2*a_1$. The figure of the contour levels shows that the fringes are still parallel to the *(Oz)* axis but has an unusual amplitude modulation along the *(Oz)* axis. This pattern depends strongly on the ratio of the beams angle a_1/a_3. At the top of Fig. 4a), the fringes intensity profiles $I(x,y=0,z=0)$ is plotted versus x as well. This profile depends strongly on the value of z as far as the main effect of the phase delay j_{nm} is to shift the entire fringes pattern in the *(Oz)* direction.

2.2 Superimposition of multiple incoherent beams pairs

We are interested here to calculate the interference field pattern produced by the superimposition of N laser beam pairs originating from the same laser source but with different time delay $(l-1)Dt$, so for the electric vectors with $l=1,\ldots,N$ we have :

$$\begin{aligned}
&\mathbf{E}_1(t) = E_0 e^{-j(\mathbf{k}_1.\mathbf{r}+j_1)} e^{-j2pnt}, \quad \mathbf{E}_2(t) = E_0 e^{-j(\mathbf{k}_2.\mathbf{r}+j_2)} e^{-j2pnt} \\
&\mathbf{E}_3(t) = E_0 e^{-j(\mathbf{k}_3.\mathbf{r}+j_3)} e^{-j2pn(t-\Delta t)}, \quad \mathbf{E}_4(t) = E_0 e^{-j(\mathbf{k}_4.\mathbf{r}+j_4)} e^{-j2pn(t-\Delta t)} \\
&\qquad\qquad \ldots \\
&\mathbf{E}_{2l-1}(t) = E_0 e^{-j(\mathbf{k}_{2l-1}.\mathbf{r}+j_{2l-1})} e^{-j2pn(t-(l-1)\Delta t)}, \quad \mathbf{E}_{2l}(t) = E_0 e^{-j(\mathbf{k}_{2l}.\mathbf{r}+j_{2l})} e^{-j2pn(t-(l-1)\Delta t)}
\end{aligned} \qquad [7]$$

Fields $\mathbf{E_n}$ and $\mathbf{E_m}$ are phase shifted by the quantity $L_{nm}=2p[(m-n-1)/2]Dt$. The resulting instantaneous field intensity at the beams crossing:

$$I \propto E_0^2 \left(N + 2\sum_{n=1}^{2N}\sum_{m>n}^{2N} |g_{nm}(\Delta t)| \cos(\mathbf{K}_{nm}.\mathbf{r} + j_{nm} + \Lambda_{nm}) \right) e^{-j2pnt} \qquad [8]$$

A function $|g_{nm}(t)|$ is introduced here to take into account the laser source temporal coherence. This function is classically known as the degree of coherence of the laser source [Lauterborn et al. 1997]. It quantifies the fringes modulation or contrast resulting from the interference of beams $\mathbf{E_n}$ and $\mathbf{E_m}$. It is a function of the time delay between the two beams. For a quasi monochromatic laser source $(Dn/v<<1)$ and beams of equal intensity the degree of coherence is equal to the fringes contrast: $|g(t)|=C(t)=(I_{max}-I_{min})/(I_{max}+I_{min})$ where I_{max} and I_{min} are the local extrema of the fringes intensity and $C(t)$, stands for the contrast function. The typical behavior of the contrast function of a quasi monochromatic sources versus the time delay is sketched in Fig. 5. The fringes contrast, i.e. the capability for the two beams to produce an interference pattern, decreases quickly when the time delay between the two beams increases, $t>>t_C$. t_C is usually defined as the time delay for which the amplitude of the contrast function has decreased in the ratio of $1/e$. A coherence length is also defined as $L_c=c\,t_c$, where c is the light velocity in the considered medium.

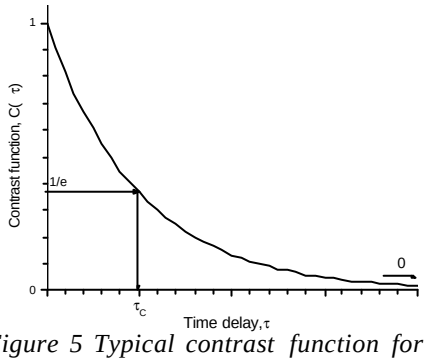

Figure 5 Typical contrast function for a quasi-monochromatic light source.

If the minimum time delay between the beam pairs is much higher than the laser source temporal coherence, $\Delta t>>t_c$, *then* their degree of coherence is then equal to zero. As a result, in Eq. 8, terms corresponding to non symmetrical beam pairs vanishe. Finally, the average intensity over the time duration $(N-1)Dt$, reduces to:

$$\langle I \rangle_{(N-1)\Delta t} \propto E_0^2 \left(N + 2\sum_{n=1}^{N} \cos(\mathbf{K}_{(2n-1)2n}.\mathbf{r}) \right) \qquad [9]$$

The net fringes pattern is simply a result of the superimposition of the fringes patterns produced by each pair of symmetrical beams. Fig 4.b) shows the fringes pattern obtained for the same parameters than in Fig. 4 a) but for two incoherent beam pairs, $|g_{12}(t)|=|g_{34}(t)|=|g(0)|»1$, $|g_{13}(t)|=|g_{14}(t)|=|g_{23}(t)|=|g_{24}(t)|=|g(Dt)| \to 0$.

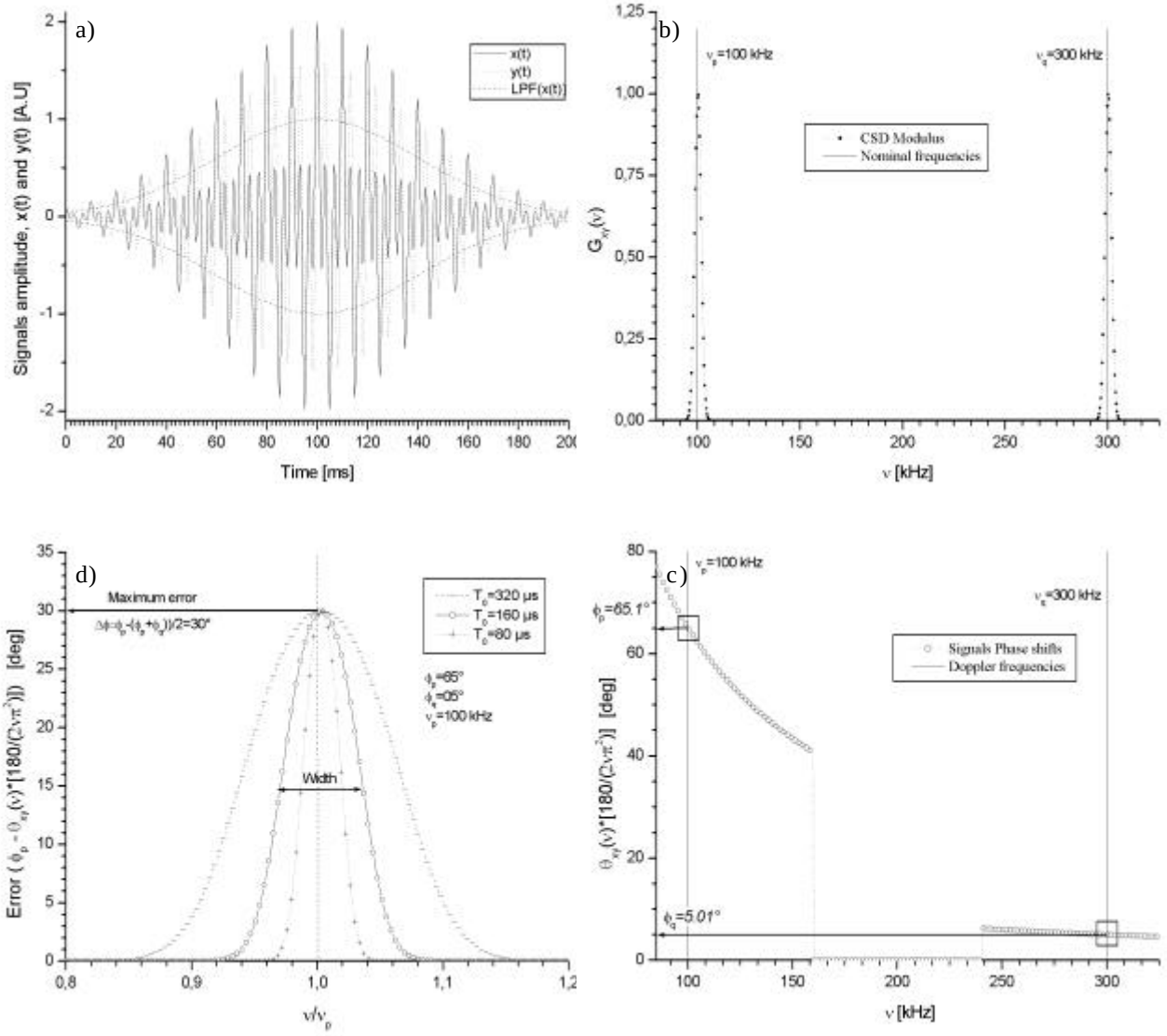

*Figure 6 Signal processing scheme a) Simulated high and low pass filtered SNIP-PDA signals produced when a particle passes through two superimposed probe volumes. The particle velocity is of 1 m/s, the effective probe volume diameter of 160µm and the fringes spacing of 3.33 and 10µm. Time series y(t) is phase-shifted in respect to x(t) by f_p=65° at frequency n_p=100kHz and by f_q=5° at frequency n_q=3*n_p. b) Modulus of the Cross Spectral Density function of the time series x(t) and y(t). c) Phase spectrum corresponding to Fig b). d) Evaluation of the error on the phase-shift estimation versus the ratio between the two Doppler frequencies. The transit time T_0 is a parameter.*

2.1 Superimposition of two cross-polarised coherent beams pairs

In the case when we have only two cross-polarized pairs of linearly polarized laser beams, with the Jone's matrix notation for polarization components, the expressions of the field vectors reduces:

$$\mathbf{E}_1(t)=E_0\begin{pmatrix}1\\0\end{pmatrix}e^{-j(\mathbf{k}_1.\mathbf{r}+j_1)}e^{-j2pnt},\quad \mathbf{E}_2(t)=E_0\begin{pmatrix}1\\0\end{pmatrix}e^{-j(\mathbf{k}_2.\mathbf{r}+j_2)}e^{-j2pnt}$$
$$\mathbf{E}_3(t)=E_0\begin{pmatrix}0\\1\end{pmatrix}e^{-j(\mathbf{k}_3.\mathbf{r}+j_3)}e^{-j2pnt},\quad \mathbf{E}_4(t)=E_0\begin{pmatrix}0\\1\end{pmatrix}e^{-j(\mathbf{k}_4.\mathbf{r}+j_4)}e^{-j2pnt} \qquad [10]$$

With the previous forms for the electric vectors, Eq. 4 reduces to:

$$\langle I\rangle_{1/n}\propto 2E_0^2\left[1+\cos(\mathbf{K}_{12}.\mathbf{r})+\cos(\mathbf{K}_{34}.\mathbf{r})\right] \qquad [11]$$

The net fringes pattern is simply the result of the superimposition of the fringes patterns produced by each pair of symmetrical beams, see Fig 4 b).

3 SIGNAL PROCESSING

The signal processing scheme used here to recover the multiple Doppler frequencies and the corresponding phase-shifts is based on the calculation of the Cross Spectral Density (CSD) function of the time series. We consider here that the signal output from each detector depends linearly on the incident scattered light onto the detector aperture.

As a first step we consider the signal output "PDA signals" from the detectors as periodic signals of a infinite time duration and without amplitude modulation, so that for one particle we have two time series $x(t)=\cos(2\pi n_D t)$ and $y(t)=\cos(2\pi n_D t-f)$, where n_D is the Doppler frequency and f the phase shift due to the particle size and refractive index. The Fourier transforms of time series $x(t)$ and $y(t)$ are respectively $X(n)=d(n-n_D)$ and $Y(n)=d(n-n_D)e^{-2j\pi nf}$, where $d(n-n_D)$ is the Dirac distribution ($d(x) \to \mu$ if $x=0$, $d(x)=0$ if $x \neq 0$). Then CSD of signals $x(t)$ and $y(t)$ is:

$$G_{xy}(n) = X(n)\overline{Y(n)} = \left|G_{xy}(n)\right| \exp\left(-jq_{xy}(n)\right) = \left[d(n-n_D)\right]^2 e^{2j\pi nf} \qquad [12]$$

The modulus of the CSD has a maximum at the signals common Doppler frequency ($\nu=\nu_D$). The phase of the CSD is equal to the signal phase-shift for $\nu=\nu_D$: $f = q_{xy}(n_D)/(2\pi n_D)$.

A more realistic PDA signal has, after high-pass filtering, the following form:

$$x(t) = Ae^{-\pi (t/t_0)^2} \cos(2\pi n_D t) \qquad [13]$$

The first factor in the right side member is a Gaussian function which accounts for the intensity distribution of the laser light in the probe volume. For usual PDA systems this function gives a good approximation for the PDA signals form provided that both the particles are small compare to the probe size and there trajectories are not too far from probe volume center. The maximum amplitude A as well as the width of the distribution (controlled with parameter τ_0) depends usually on a large number of parameters such as the particle properties (size, shape and refractive index), the detector aperture size and shape, the laser power,… In Eq. 13, the second factor accounts for the interference phenomenon observed onto the detectors when a particle is passing trough the probe volume. The Fourier transform of $x(t)$ reads:

$$X(u) = \frac{At_0}{2}\left(e^{-\pi[(n-n_D)t_0]^2} + e^{-\pi[(n+n_D)t_0]^2}\right) \qquad [14]$$

If we consider now a second PDA signal $y(t)$ similar to $x(t)$ but phase-shifted by the quantity f, its Fourier Transform is simply equal to $Y(n) = X(n)e^{2j\pi fn}$. Then the CSD of the two signals reads

$$G_{xy}(n) = = \frac{A^2 t_0^2}{4}\left(e^{-\pi[(n-n_D)t_0]^2} + e^{-\pi[(n+n_D)t_0]^2}\right)^2 e^{2j\pi fn} \qquad [15]$$

Here again the signal Doppler frequency is equal to the frequency where the modulus of the CSD is maximum (i.e. the Gaussian distribution $\exp[-\pi(\nu-\nu_D)\tau_0]^2$ is maximum for $\nu=n_D$). Knowing n_D the phase shift between the two signals can be deduced from the CSD phase spectrum. The only difference between the previous ideal case appears in the frequency bandwidth of the peaks which depends on the particle transit time τ_0.

In the case we have N incoherent superimposed probe volumes with the same diameter and the same intensity, SNIP-PDA signals have the following forms:

$$\begin{aligned} x(t) &= Ae^{-\pi (t/t_0)^2}\left(\cos(2\pi n_1 t) + \cdots + \cos(2\pi n_n t)\right) \\ y(t) &= Ae^{-\pi (t/t_0)^2}\left(\cos(2\pi n_1 t)e^{-2j\pi f_1 n} + \cdots + \cos(2\pi n_n t)e^{-2j\pi f_n n}\right) \end{aligned} \qquad [16]$$

in the positive frequency domain, the CSD of these two series reads,

$$G_{xy}(n) = = \left(\frac{At_0}{2}\right)^2 \left(e^{-\pi[(n-n_1)t_0]^2} e^{2j\pi nf_1} + \cdots + e^{-\pi[(n-n_n)t_0]^2} e^{2j\pi nf_n}\right) \sum_{n=1}^{N} e^{-\pi[(n-n_n)t_0]^2} \qquad [17]$$

Thus for SNIP-PDA signals the CSD amplitude spectrum exhibits a multiple peak pattern whereas the phase spectrum exhibits a multiple plateau pattern. Provided that there is no overlapping of the peaks, this signal processing scheme can be use to recover all the desired quantities (ν_1, ϕ_1), (ν_3, ϕ_3),…, (ν_{2l-1}, ϕ_{2l-1}) from only two SNIP-PDA signals.

The relevance of this signal-processing scheme can be evaluated from Fig. 6. Fig 6a) shows simulated High Pass and Low Pass Filtered PDA signals (HPF, LPF), produced when a particle passes through two superimposed proves volumes. Eq. 13 is used here with $A=0$ and $t_0=100\mu s$ which corresponds, for instance, to a particle velocity of $V=1$ *m/s*, to an effective probe volume diameter of $160\mu m$ and to a fringes spacing $i_p=10\mu m$ and $i_q=i_p/3$. Time series $y(t)$ is phase shifted in respect to series $x(t)$ by $f_p=65°$ at the Doppler frequency $n_p=V/i_p=100kHz$ and by $f_q=5°$ at the Doppler frequency $n_q=3*n_p=300kHz$. The amplitude spectrum and phase spectrum, $|G_{xy}(n)|$ and $q_{xy}(n)$, of the CSD of $x(t)$ and $y(t)$ calculated by using Eq. 15 re shown in Figs. 6 b) and Fig. 6 c). $|G_{xy}|$ exhibits two peaks, each of which is centered on the nominal Doppler Frequencies n_p and n_q. From the CSD phase spectrum one can geometrically extract the two phase-shifts corresponding to the two peaks in the amplitude spectrum, and found 65.1° and 5.01°. These phase-shifts are almost equal to the nominal phase shifts f_p and f_q.

Without any frequency shift of the laser beams (with Braggs' cells or rotating transmission gratings) the two frequencies n_p and n_q are always supposed to be clearly distinct ($n_p/n_q=i_p/i_q>1$). They have nevertheless a certain frequency bandwidth. This bandwidth is related to the particle transit time in the probe volume, i.e. $T_0=2t_0\sqrt{2/p}$, the probe diameter being defined at $1/e^2$.

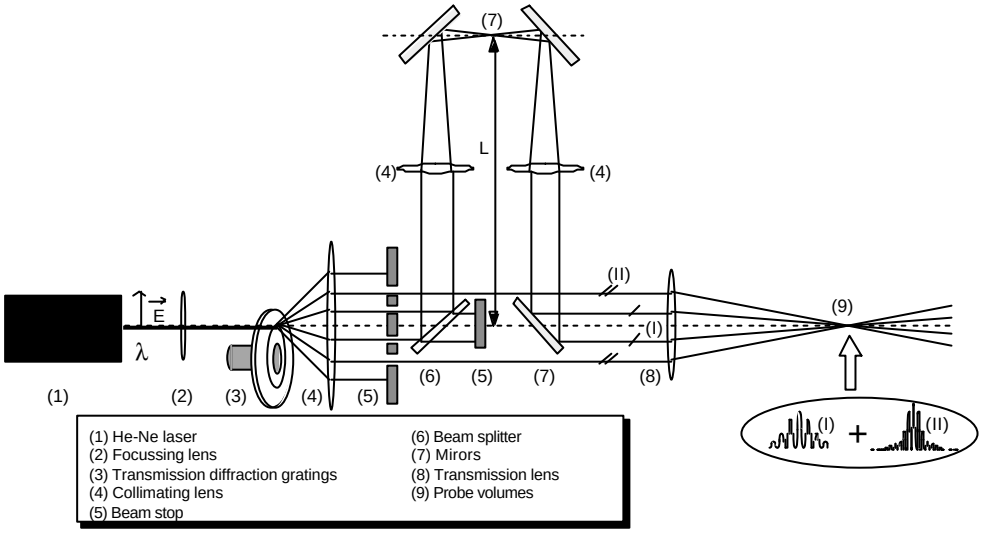

Figure 7 System A: experimental setup for a production of two non coherent superimposed probe volumes with a single low coherence laser source. The path of beam pair (I) is increased by the length 2L in respect to the path of the beam pair (II).

If the laser beams are frequency shifted then the frequency n_p and n_q are not obligatory in the same ratio than the probe volumes fringes spacing. One can imagine that the probe volume with the smaller fringes spacing i_q (i.e. largest phase-diameter conversion factor) is frequency shifted in order to obtain Doppler signal with a frequency close to the one produced by the other probe so that we have finally, $n_q \approx n_p$. The interest to do that would be for instance to limit the dynamic ranges of the Doppler signals.

To evaluate this effect (i.e. the overlapping of the peaks in the CSD spectrum frequency domain) we restrict our analysis to the two closest Doppler Frequencies in times series $x(t)$ and $y(t)$, namely n_q and n_p, so that only two terms have to be considered:

$$G_{xy}(n_p) = \left(\frac{At_0}{2}\right)^2 \left(e^{2jpnf_p} + e^{-p\left[(n_p-n_q)t_0\right]^2} e^{2jpnf_q}\right)\left(1+e^{-p\left[(n_p-n_q)t_0\right]^2}\right) \qquad [18]$$

In Fig. 6 d), the difference between the nominal phase f_p and $q_{xy}(n)$ at the peak maximum of $|G_{xy}(n_p)|$is plotted versus the frequency ratio n/n_p. Note that $n/n_p=1$ when $n_q=n_p$, i.e. the two peaks overlaps completely. The transit time T_0 of the signals $x(t)$ and $y(t)$ acts as a parameter. In the case where $T_0=160\mu s$, see Fig. 5. a-c), the error in the phase shift estimation can be neglected when $\nu_p/n_q>1.08$ or $n_p/n_q<0.92$. The error is maximum when $n_p/n_q=1$ and raises to the value of $30°$. This particular value is in fact the average value of the two phase-shift f_p

and f_q, $f_p-(f_p+f_q)/2=65-(65+5)/2=30°$. A decreasing particle transit time increases the peak frequency bandwidth and then the possibility for peaks overlapping. Note that the worst case, T_0=80 µs, corresponds to extremely low modulated signals.

4 EXPERIMENTAL VALIDATION TESTS

4.1 Experimental setups

Following the considerations of the section 3, three systems to produce non interfering superimposed probe volumes have been investigated with two types of reception units.

System A: single low coherence laser source with a retardation line

The first system takes advantage of the limited coherence time of a *2.5mW* He-NE Laser from Melles Griot, see Fig 7. According to the manufacturer technical notes, this laser has a longitudinal mode spacing of *822 MHz*, so that its coherence length is of $L_c \approx 0.35$ m which corresponds to a coherence time of $\tau_c \approx 1.2$ ps.
The laser beam output is directed onto a rotating transmission diffraction grating and then collimated by a spherical lens. A beam stop is use to stop all the beams of order different from ±1 and ±2. A beam splitter separates beams ±1 in two parts. One part is directed to a beam stop, the other one is directed to an optical system (retardation line) which allows to control the additional path length *2L* and to maintain the beams divergence (two lens of equal focal length are used for this purpose). At the output of this system, this beam pair (I) is redirected in order to be parallel to the two beams pair (II). Finally, the probe is formed by focussing the four laser beams by a transmission lens.

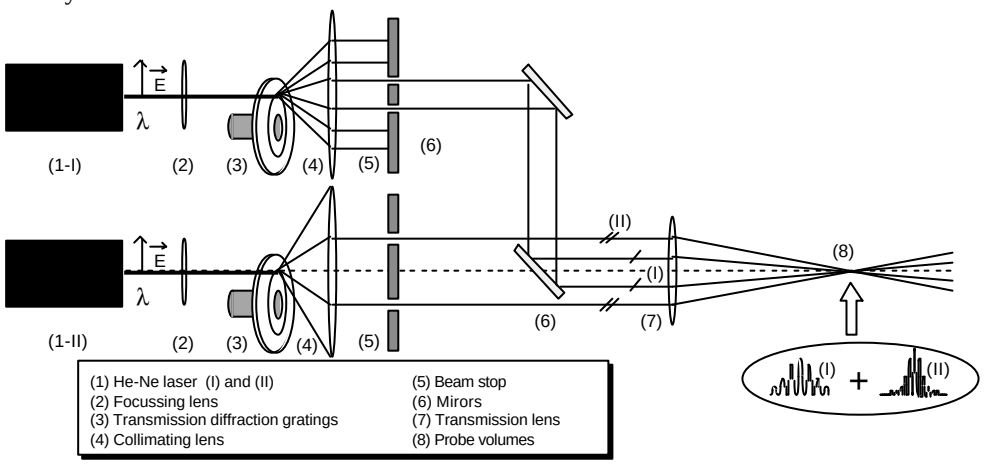

Figure 8 System B: experimental setup for a production of two non coherent superimposed probe volumes from two independent laser sources with the same wavelength and polarization state.

From practical considerations, in our experiments we were limited to a maximum addition path length of *2L »2 m* (so that the condition $2L>L_c$ was satisfied as far as we have $2L/L_c$ *»5.7*). Nevertheless, this additional path was found to be not enough to totally avoid interference between the two beam pairs. In fact, a low frequency variations of the fringes pattern could be observed during the experiment. In a future work, this solution will be further investigated with a shorter coherence length laser source (a low coherence laser diode) as well as with a retardation line based on optical fibers.

System B: two independent laser sources

A second system has been developed of the basis on the utilization of two different laser sources, see Fig. 8. This system is a limit case of the *System A*. In fact in *System B* the two lasers sources have a priori no phase relationship so that it is almost equivalent to *System A* when the additional path length tends to infinity ($g(Dt) \to 0$ when $L \to \mu$) [Lauterborn et al., 1997].
The beams of the order ±1 of each systems were aligned to be parallel and focussed at the same location by a single transmission lens. For the two beam pairs *(I)* and *(II)* the diffraction gratings tracks were different to ensure different beam spacing and then fringes spacing. This solution works perfectly and we did not notice any effects coming from interference between the two pairs of beams.

System C: two cross-polarized probes

The last experimental setup is based on the superimposition of cross-polarized pairs of beams, see Fig 9. The output of a 10mW linear polarized He-Ne laser is directed on a rotating transmission diffraction gratings. The diffracted beams are collimated by a spherical lens. A beam stop is then use to stop all beams order different from ±1 and ±3 (±2 in Figure 9) . The intensity of the diffracted beams ±1 is much higher than the intensity of higher order beams so that this can lead to some difficulties for signal detection. Thus, a variable neutral density filter is placed along the propagation of the beams ±1 to decrease their intensity up to the intensity of the other beams pair. Afterwards a single half-wave retardation plate is used to turn to 90° the polarization plan of beam pair (I) in respect to the polarization plane of the beam pair (II). Finally, the probe is a summation of two cross-polarized probes with different fringes spacing.

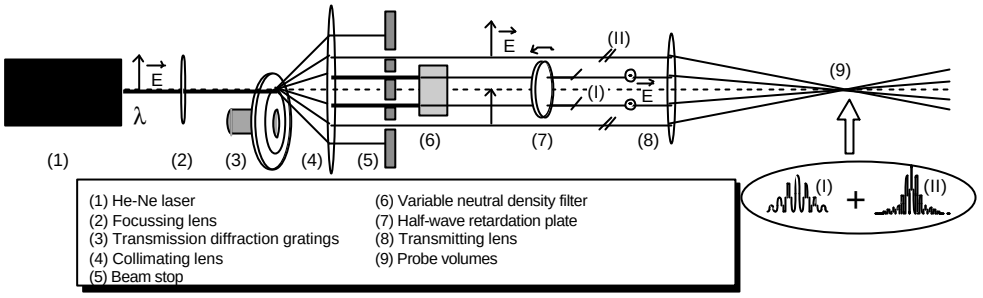

Figure 9 System C: experimental setup for the production of two cross-polarized non interfering superimposed probe volumes from a single laser source.

4.2 Experimental results

The principle of the proposed technique has been validated both on the sizing of spherical glass beads and cylindrical metallic wires.

System (B) for the sizing of glass beads:

A emission unit based on the working principle of *System B*, see Fig. 8, was used to produce two incoherent superimposed probes with a diameter of *320µm* at $1/e^2$. For signal detection a reception unit from an Aerometrics [TSI, inc.] system was used. This classical PDA system has three detectors ($\psi_{1,2}=\pm 4.1$, $\psi_3=\pm 1.57°$). It was located in the forward scattering domain at an off axis-angle of 30°. The optical parameters of the SNIP-PDA (*System B* plus the Aerometrics reception unit) lead to the following phase-shift diameter conversion factors $C_{12,(I)}= 1.544°/\mu m$ and $C_{12,(II)}= 4.973°/\mu m$ (so that the fringes spacing was in the ratio ≈3). For the standard Aerometrics system (its own emission and reception units), the corresponding conversion factors were of $C_{13} =1.534°/\mu m$ and $C_{12}= 4.973°/\mu m$.

Fig. 10 shows the projected image of the fringes pattern in the *(Oxy)* plane. Fig 10 a) is obtained when beams *(II)* were blocked before to form the probe volume and Fig 10 b) when beams *(I)* were blocked . In Fig 10 c) we observe the superimposition of the fringe patterns from beams *(I)* and *(II)*. This last pattern clearly exhibits a multiple frequency structure. It looks to be similar to the one calculated in Fig 4b) whatever the projection planes are not identical in the two figures. A second basic experiments has been carried out with a single glass bead (*m»1.51*) glued on a needle which was itself fixed on a turning wheel so that we were able to control the particle trajectory and velocity in the probe volume. The bead shape and diameter were controlled and measured with an optical microscope. Its diameter was found to be equal to *≈190 µm*. Fig.10 a) a typical SNIP-PDA signal recorded during the experiment is presented. The modulus and the phase spectrum of the CSD of this signal (the second signal is not presented here) are plotted bellow in Fig. 10 b) and Fig. 10 c) respectively. In Fig. 10 b) the two peaks are well defined so that the signals phase-shifts can be easily be deduced from the CSD phase spectrum: $f_{12,(I)}=135°$ at the low Doppler frequency (probe volume with largest fringes spacing) and $f_{12,(II)}=229°$ at the high Doppler frequency (probe volume with smallest fringes spacing). Knowing the two conversion factors the particle size is found to be successively of *204.4 µm* and *190.8 µm* (a phase jump of *2*2p* has been added to the phase-shift f_{II}). These values, averaged over *1000 samples*, are in a good agreement with the expected value.

In Fig. 12 the measurement of the size distribution of glass beads falling down from a vibrating tank is considered. The glass beads were previously sieved to be in the nominal size range: 100-160µm. A typical size distribution obtained with the full Aerometric system is shown in Fig 12 a). The corresponding measurement obtained with SNIP-PDA is plotted in Fig 12 b).

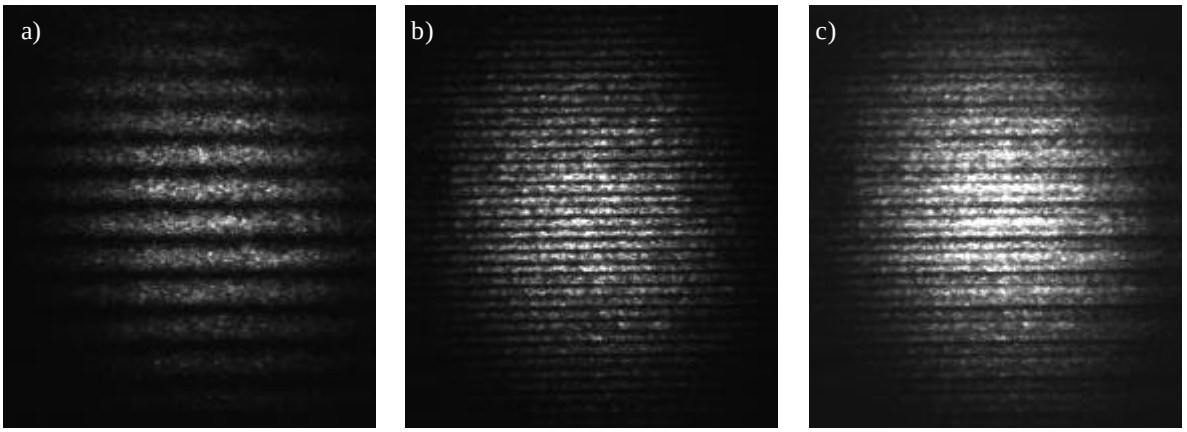

Figure 10 Image of the projection of the probe volume fringes pattern in plane (Oxy) : a) beams pair (I) only, b) beams pair (II) only, c) beams pairs (I) and (II), a superimposed multiple frequency pattern is observed.

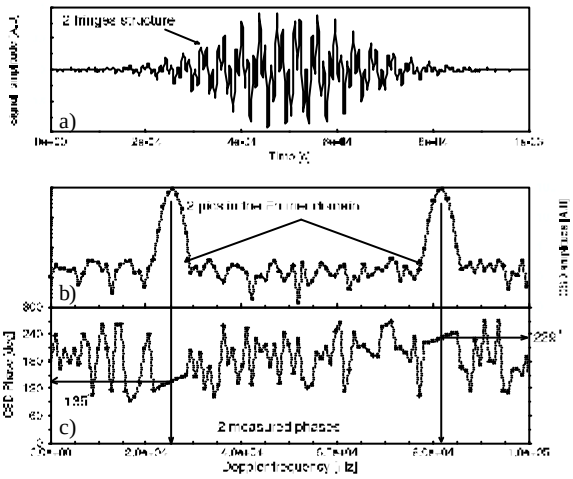

Figure 11 a) Experimental signal recorded when a 190 µm glass bead is passing trough the probe volume of System B. Its CSD spectrum is shown in b) the modulus and in c) the phase.

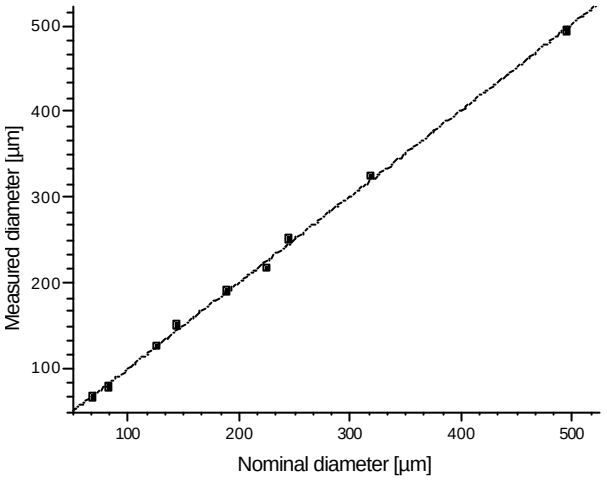

Figure 13 Comparison between the nominal size of metallic wires and their measured size with System C.

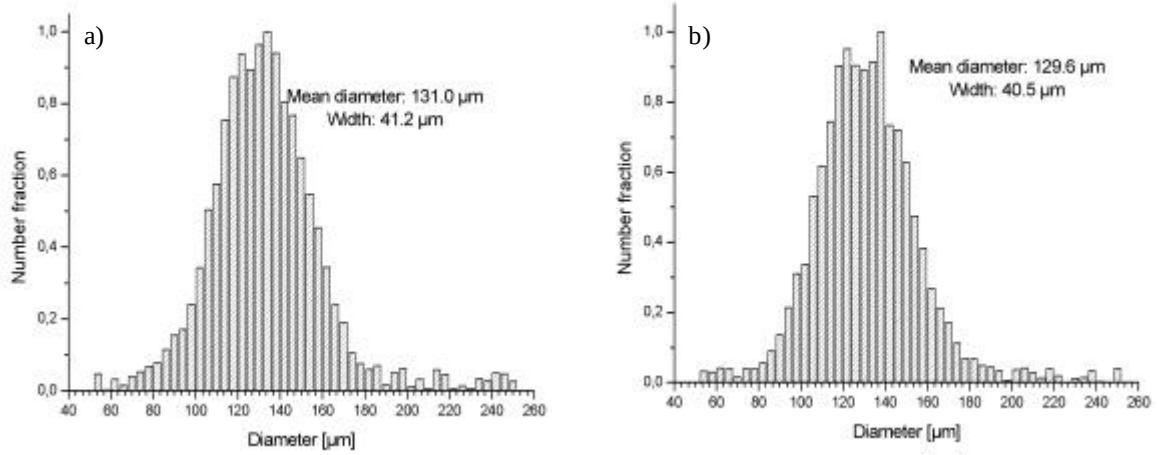

Figure 12 Measured size distributions with a) a classical phase Doppler Anemometer and b) the SNIP-PDA, System B, of sieved glass beads falling down from a vibrating tank by gravity.

For both systems the statistics have been performed over 10000 validated samples. The SNIP-PDA signals were treated with a special acquisition and processing software developed by ourselves on the basis of the signal

processing scheme described in section 3. Note that that there is almost no significant differences between the two size distributions and their statistical moments.

System (C) for the sizing of metallic wires:

A second system based on the use of cross-polarized laser beams, *system C*, and backwards collections units have been investigated for the sizing of small diameter metallic wires. The two single detector reception units were built by ourselves and placed in the backward scattering region at $y_{1,2}=\pm 170°$. Beam pairs *(I)* and *(II)* were used to produce a superimposed probe volume giving rise to a beam angle ratio of $\alpha_I/\alpha_{II}=1.835°/0.454°\approx 4$. The probe volume diameter was of $600\mu m$ at $1/e^2$. The metallic wires were made of pure copper and they were fixed successively in the probe volume. Copper has a complex refractive index in the visible domain of $m=0.88-0.46j$. Different wires diameters were measured. Their nominal diameter was controlled with a high precision micrometer of $\pm 1\ \mu m$ resolution. Fig. 13, shows a comparison between the nominal values for metallic wires diameters and the ones measured with the SNIP-PDA over 5000 samples. The two measurements are in a good agreement over all the size range.

5 CONCLUSION

In the present work an alternative solution is proposed to avoid the need of a third detector in Phase Doppler systems. The proposed solution consists in the Superimposition of Non Interfering Probes (SNIP) in order to obtain multiple frequency Doppler signals and to extract, for each Doppler frequency presented in these signals, a phase-shift that can be related to the particle diameter.

The principle of three optical systems which allows to produce SNIP are introduced. The first one, uses a single low coherence laser source and a retardation line. From practical consideration as well as for practical applications it is probably the more promising system, although it has not be tested successively in the present work due to our limited experiments facilities. Nevertheless it has been validated in the equivalent limit case of an infinite retardation line length (i.e. the two independent laser sources used in the second system). The last system is based on the use of a single laser source and cross-polarized probes. It is obviously the most simple system to develop and reliable size measurements have been already performed with this system as well as with the second system. Nevertheless, its applicability is restricted to some particular applications. In fact the working principle of this system assumes that the light scattered in the detectors direction from a particle located in a probe volume same polarization state than incident lasers beams used to produce the considered probe. This condition can not be fulfilled for of all kind of particles materials, size ranges and collection angles.

The principle of a signal processing scheme for the treatment of SNIP-PDA signals has been introduced, it is based on the calculation of Cross Spectral Density function.

According to the authors the SNIP-PDA technique has some particular advantages when compared to the classical PDA technique for the sizing of small particles or fibers (D<10µm) and possibly for the diagnosis of irregular particles. These features will be described in a further work.

6 ACKNOWLEDGEMMENT

The authors are grateful to the French National Center for Scientific Research and the Bulgarian Academy of Sciences for providing financial support for this work (project CNRS-BAS n°6617).

7 REFERENCES:

Durst F., Melling A. and Whitelaw J.H., Principles and practice of laser-Doppler anemometry, Academic Press, London, 1981

Lauterborn W., Kurz T., and Wiesenfeldt M., Optique Cohérente, Masson, Paris, 1997.

Naqwi A. and Durst F., "Light scattering Applied to LDA and PDA Measurements, Part1: Theory and Numerical treatments", *Part. and Part. Syst. Charact*., V8, pages 245-258, 1988.

Naqwi, A. , Sizing of Irregular Particles Using a Phase Doppler System, *Part. and Part. Syst. Charact*., V13, N6, 1996.

Onofri F., Etude numérique et expérimentale de la sensibilité de l'interféromètrie phase Doppler à l'état de surface des particules détectées, accepted for presentation to the 7ème Congrès Francophone de Vélocimétrie Laser, Marseille, Sept. 2000.

Tropea C., Xu T-H., Onofri F., Gréhan G., Haugen P., Dual-Mode Phase Doppler Anemometer, *Part. and Part. Syst. Charact*.,V13, pages 165-170,1995.

TSI Incorporated, 500 Cardigan Road, Saint Paul, 55126 MN, USA.